

Shear Capacity of Self-Compacting Concrete Beams provided by External Steel Plate using Z Stirrups

Douaa Kasim

Department of Civil Engineering, College of Engineering, Mustansiriyah University, Baghdad, Iraq
dzaid3034@uomustansiriyah.edu.iq (corresponding author)

Wissam Alsaraj

Department of Civil Engineering, College of Engineering, Mustansiriyah University, Baghdad, Iraq
wkaswkas5@gmail.com

Received: 10 October 2024 | Revised: 4 November 2024 | Accepted: 4 December 2024

Licensed under a CC-BY 4.0 license | Copyright (c) by the authors | DOI: <https://doi.org/10.48084/etasr.9218>

ABSTRACT

The stirrups are the primary factor that resists the shear forces, while other parameters like aggregates and dowels contribute less than 7% of the shear strength. Shear connectors transmit the shear forces in composite beams between steel parts and concrete, and these connectors can be utilized as vertical legs to assist the stirrups in their performance. The results indicate that decreasing the shear span to effective depth (a/d) ratio from 3 to 2.5 led to a 24% increase in the crack load and a 16% increase in the maximum load value. Additionally, the shear connectors have a significant effect on increasing the shear capacity, and this effect becomes more pronounced as their lengths increase, effectively replacing the function of the stirrups. Furthermore, the change in the shape of the stirrups does not significantly affect the shear capacity, and the decrease in endurance can be compensated by reducing the distance between the stirrups. It was also observed that the horizontal parts of the stirrups may have a limited and negligible effect, suggesting that the stirrups could potentially be replaced by I-shaped alternatives.

Keywords-bendable concrete; self-compacting concrete; external steel plate; Z stirrups; composite beams

I. INTRODUCTION

Composite beams combine steel and concrete to provide higher load capacity, ductility, stiffness, and cost-effectiveness compared to non-composite or steel beams. This leverages the advantageous properties of materials, such as the steel's tensile strength and the concrete's compressive strength [1-4]. Self-Consolidating or Self-Compacting Concrete (SCC) is a highly flowable, non-segregating concrete that can spread and fill the formwork under its own weight. Shear connectors linking the steel beam and concrete slab are crucial for the composite member construction. They are, also, critical for the seismic performance of composite structures, providing the necessary shear connection for composite action and distributing the forces [4-6]. The impact of shear helical rings on Reinforced Concrete (RC) beams when subjected to static load and four-point bending has been investigated determining the maximum beam load and crack patterns [7]. Twenty-four models of 2 concrete beam types were analyzed: 12 SCC beams and 12 compressed concrete beams. Both variants featured a vertical ring reference beam and continuous helical ring beams. The beams were designed to resist shear failure and bending. The variables examined included the shear space-to-depth ratio. The findings indicate that helical rings enhance the shear capacity

by approximately 5%, while increasing the shear area-to-depth ratio amplifies the effect of the helical rings. Additionally, helical rings are more cost-effective than separate rings, as they overlap and reduce crack widths. Eight concrete beam models were tested, reinforced with external steel plates instead of shear stirrups of the same size, and length, height, and width of 1000×200×150 mm [8]. The beams were reinforced by applying steel plates externally, with the plate area matching the missing area after the beams were loaded until the first crack occurred. Based on the plate thickness, the beams were divided into three groups, namely 1 mm, 1.5 mm, and 2 mm. The reinforced beams, particularly those using screws with epoxy to attach the plates, exhibited significant strength improvements. The maximum load capacity of the test specimen was higher than that of the reference beam without internal shear stirrups, ranging from 75.46% to 106.13% of the reference beam's ultimate load. Additionally, the test specimen's performance showed good agreement with the control beam containing shear reinforcement, reaching between 76.06% and 89.36% of the ultimate load.

The Flamingo technique was investigated, an alternative shear reinforcement technique which utilizes prefabricated components instead of traditional vertical stirrups [9]. The

study employed five RC beams with dimensions of $200 \times 300 \times 1800$ mm, comprising two reference beams, including beams with stirrups and without stirrups, and three beams utilizing the Flamingo technique. The Flamingo beams had free ends, a constant inclination angle of 45° , and a fixed effective depth length of 80% and 60% mm. This research aimed to determine the impact of changing the diameter on the performance of the Flamingo technique. The diameters evaluated were 6, 8, and 10 mm. The study findings revealed an enhancement in the shearing capacity of the beams by 13.8%, 25%, and 40.55% compared to the reference beam. Additionally, the end cracks and the behavior of the cracked beam were also improved. When compared to the control beam (RCWS), the FD6, FD8, and FD10 beams exhibited decreases in deflection of 32.8%, 11.3%, and 14.8%, respectively.

Shear connectors transmit the shear forces in composite beams between the steel components and the concrete, and therefore these connectors can be utilized as vertical legs to assist the stirrups in their performance. The vertical legs of the stirrups, the area perpendicular to the forces exerted, are the main parts responsible for carrying those forces. In this paper, the researchers will use Z-shaped stirrups instead of the traditional U-shaped stirrups in order to reduce the amount of the rebar utilized and ease the process of forming it. This approach is expected to provide benefits in terms of material efficiency and construction simplicity compared to the conventional U-shaped stirrups.

II. EXPERIMENTAL PROGRAM

Four groups consisting of ten RC beams were constructed to undergo monotonic testing under one-point and two-point loads. Additionally, two RC beams were produced for comparison purposes, with the objective of utilizing a new technique of shear reinforcement. The beam details are presented in the Table I and Figure 1. All the beam specimens shared the same dimensions, including an overall length of 1200 mm and a rectangular cross-section with a width of 150 mm and a depth of 220 mm.

The structural beams are provided by an external steel plate with 2 mm thickness along the longitudinal axis of the beam and are connected to the main beams by T-shape shear connectors made locally at the laboratory. The variables which were studied in this paper include the spacing between the Z stirrups, length of flange of the Z stirrups, length of the shear connectors that connected the steel plate to the main beams, and a/d .

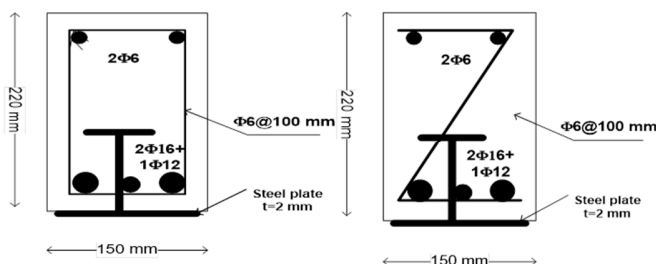


Fig. 1. Detailed illustration of beams' reinforcement.

TABLE I. DETAILS OF TESTED BEAMS

Beam No	Shear connector length (mm)	a/d	Shear reinforcement			
			Group	Spacing (mm)	Y (mm)	X (mm)
B1	WO	3.0	Ref.1	100	185	110
B2	100	3.0	Ref.2	100	185	110
B3	100	3.0	A	80	185	110
B4	100	3.0	A	120	185	110
B5	100	3.0	B	100	185	80
B6	100	3.0	B	100	185	50
B7	150	3.0	C	100	185	110
B8	180	3.0	C	100	185	110
B9	100	2.7	D	100	185	110
B10	100	2.5	D	100	185	110

III. MATERIALS

A. Cement

Ordinary Portland cement (CEM I 42.5R) was used in compliance with the requirements of the Iraqi Specification No. 5/2019 [10].

B. Fine and Coarse Aggregate

Natural fine aggregate with a fineness modulus of 2.87 and falling within zone No. 2 was utilized. Crushed gravel, with particle sizes ranging from 5 to 12 mm, was incorporated into the concrete mix to enhance the structural strength through the interlocking of the angular particles. The use of coarse aggregate in SCC aims to achieve a desirable flow. The grain size distribution and physical characteristics of this aggregate complied with the requirements outlined in the Iraqi Specification No.45/1984 [11] and its revisions.

C. Fillers

The nature and quantity of fillers utilized aims to address the strength and durability requirements, mitigate the excessive heat generation, limit the segregation and bleeding of the mixture, and enhance concrete performance while moderating workability.

D. Superplasticizer

The super plasticizer that was deployed in the preparation of concrete is Glenium 51, manufactured in the United Arab Emirates with a PH value of 6.8, a light brown color, and free of chlorine.

E. Steel Reinforcing Bars

The primary tensile reinforcement consisted of two $\text{Ø}16$ mm and one $\text{Ø}12$ mm to ensure shear failure of the section, supplemented by two $\text{Ø}6$ mm longitudinal smooth steel bars, employed as a holding mechanism for the transverse reinforcement. The transverse reinforcement comprised $\text{Ø}6$ mm bars spaced at 100 mm centers, with the exception of B2 and B3, which had 80 mm and 120 mm spacings, respectively. The longitudinal and transverse steel reinforcement were designed in accordance with ACI318-19 [12].

F. Steel Plates and Shear Connectors

The plate thickness must be equal to or less than the thickness at balanced load conditions and the maximum thickness to ensure a ductile flexural failure [13].

$$\frac{b_p}{t_p} \geq 50 \tag{1}$$

The study utilized steel plates with a thickness of 2.0 mm, a width of 145 mm and a total length of 1200 mm. Homemade shear connectors were fabricated using deformed steel rods with a diameter of 12 mm. These shear connectors had a T-shaped configuration, with an 88 mm stem and an 80 mm flange, resulting in a total height of 100 mm. The shear connectors were employed in most of the beams, while some beams incorporated taller shear connectors of 150 mm and 180 mm. These shear connectors were spaced at 200 mm center-to-center intervals to facilitate the transfer of forces from the concrete to the steel plate, with a measurement accuracy of 0.01 mm. One shear connector was positioned at the beam's center, and another was placed under the point loads, as depicted in Figure 2.

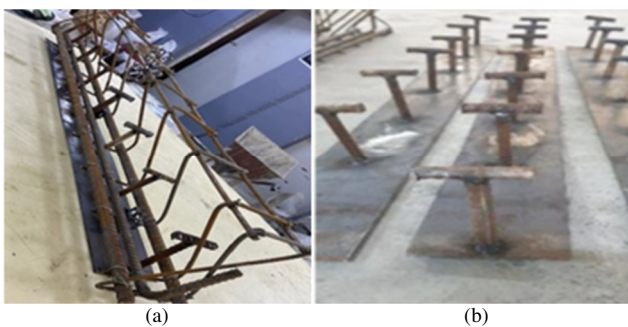


Fig. 2. (a) Steel plate and (b) shear connectors.

IV. MIXTURES

The mixes used to cast the specimens were based on previous research, as well as the tabulated, modified, and trial mix data until the following SCC mix proportions were achieved, with a content ratio of 1:1.57:1.94 by weight and with a water-to-powder ratio of 0.34 [14]. The mix design method for SCC must meet the requirements of the passing ability, filling ability, and segregation resistance [15].

TABLE II. SCC MATERIAL WEIGHT QUANTITIES

Cement (kg/m ³)	Sand (kg/m ³)	Gravel (kg/m ³)	Limestone (kg/m ³)	Super Plasticizer (l/m ³)	Water (l/m ³)
425	670	825	150	10	150

V. CURING

All beams and specimens were enclosed in plastic bags to prevent water evaporation and mitigate surface shrinkage. The beam specimens were demolded 48 hours later, while the cylinders, cubes, and prisms were demolded after 24 hours. The normal concrete underwent water curing, whereas the SCC specimens were subjected to ambient curing at laboratory temperature until the testing day.

VI. RESULTS

A. Mechanical Properties

1) Fresh Properties

To verify that the mix meets the SCC requirements, the fresh property results must fall within the specified limitations. In this investigation, two tests were conducted: the T50 slump flow test and the slump flow test, as well as the V-funnel test and the V-funnel test at T5 min. The results of these tests are presented in Table III and are compared to the relevant limitations of EFNARC and ACI-237 [15, 16].

2) Hardened Properties

The mechanical properties of the concrete used in the casted beams, including specified compressive strength (*f_c*), characteristic strength (*f_{cu}*), modulus of rupture (*f_r*), splitting tensile strength (*f_t*), and modulus of elasticity (*E_c*), are portayed in Table IV and are compared to the values suggested by the American Concrete Institute (ACI) 318M [12].

$$f_r = 0.62\sqrt{f'_c} \tag{2}$$

$$f_t = 0.56\sqrt{f'_c} \tag{3}$$

$$E_c = 4700\sqrt{f'_c} \tag{4}$$

TABLE III. SCC FRESH PROPERTIES TEST RESULTS

Tests	T50 Slump Flow (sec)	Slump Flow (mm)	V-Funnel (sec)	V-Funnel at T5min (sec)
SCC	4.5	740	8.5	9
EFNARC Limitations	2.0-5.0	650-800	8.0-12.0	3
ACI-237 limitations	2.0-5.0	450-760	-	-

TABLE IV. MECHANICAL PROPERTIES RESULTS

Compressive Strength		
<i>f_{cu}</i> (MPa)	<i>f_c</i> (MPa)	<i>f_c/f_{cu}</i>
44.1	37.5	0.85
Tensile Strength		
<i>f_t</i> (Mpa)	<i>f_t</i> (MPa) (ACI)	
3.42	3.43	
Modulus of Rupture		
<i>f_r</i> (MPa)	<i>f_r</i> (MPa) (ACI)	
4.50	3.80	
Modulus of Elasticity		
<i>E_c</i> (MPa)	<i>E_c</i> (MPa) (ACI)	
3145	2878	

B. Shear Response of SCC Beams

This section examines the load-deflection (*P-δ*) relationship, load capacity, failure modes, and cracking patterns of ten reinforced SCC beams subjected to different levels of monotonic loads [17]. The loads were applied incrementally at a rate of approximately 10 kN/min until failure. The complete results are depicted in Table V. Figure 3 displays the relationship between cracking and the ultimate applied load for the experimental groups, which varied according to the studied parameter. The results demonstrate a reduction of approximately 19% in the shear capacity of the beams when the stirrups were changed from U-shaped to Z-shaped. However, this reduction may be mitigated by decreasing the spacing between the Z-shaped stirrups or increasing the length of the shear connectors.

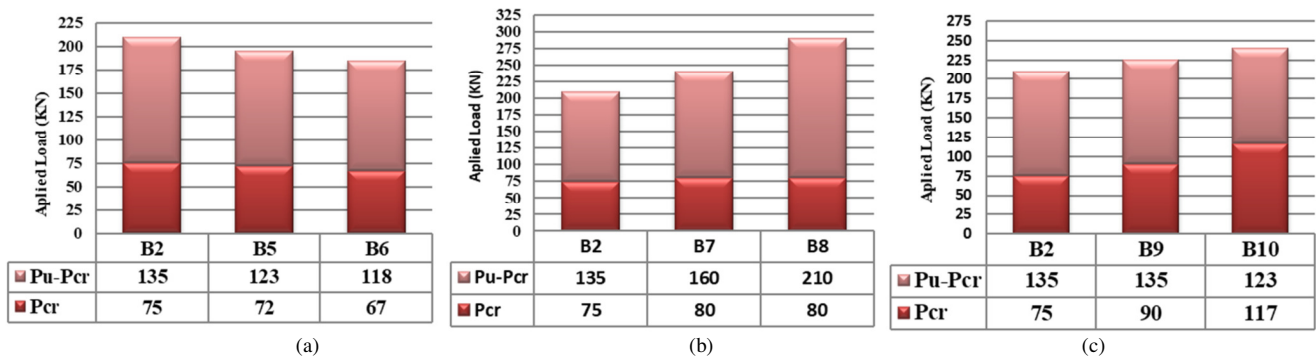


Fig. 3. Relation between cracking and ultimate applied load for beams (a) B2, B5, and B6, (b) B2, B7, and B8, and (c) B2, B9, and B10.

TABLE V. EXPERIMENTAL PROGRAM RESULTS

Group	Beam No.	Pcr (KN)	B2 (%)	Δcr (mm)	B2 (%)	Pu (KN)	B2 (%)	Δu at Pu (mm)	B2 (%)
-	B1	72	-4	0.74	-42	250	19	7.95	-2
-	B2	75	0	1.28	0	210	0	8.1	0
A	B3	80	7	1.23	-4	225	7	9.45	17
	B4	65	-13	1.58	23	170	-19	10.95	35
B	B5	72	-4	1.25	-2	195	-7	7.35	-9
	B6	67	-11	1.35	5	188	-10	7.95	-2
C	B7	80	7	1.43	12	240	14	12.75	57
	B8	86	15	1.05	-18	290	38	12.3	52
D	B9	85	13	1.25	-2	225	7	7.95	-2
	B10	93	24	1.2	-6	240	14	9.45	17

Figure 4 depicts the relationship between the applied load and the deflection at the mid-span point for the groups, considering the variables. The increased ultimate load of the SCC beams in group A is attributed to the enhanced contribution of the transverse reinforcement to shear strength when the spacing between the Z-stirrups was reduced. Conversely, the slight decrease in the ultimate load of the SCC beams in group B is due to the reduced stiffness of the beams, resulting from the decreased flange length of the Z-stirrups. In contrast, the transverse reinforcement strength contribution remained constant due to the unchanged spacing between the Z-stirrups. The increased ultimate load of the SCC beams in group C is associated with the enhanced contribution of the shear connectors to shear strength, while the transverse reinforcement strength contribution remained constant due to the constant spacing between the Z-stirrups. The increased shear capacity of the RC beams equipped with external steel plates, connected using shear connectors, is a well-established fact that is attributed to the increase in the length of these connectors. In group D, the decreased shear span ratio led to an increase in the ultimate load of the SCC beams.

C. Ductility, Stiffness, and Energy Absorption

Figure 5 presents the ductility ratio, initial and service stiffness, and toughness characteristics of the beams. The ductility is a crucial property of concrete structural members, defined as the ability to undergo substantial deformations without experiencing brittle failure. Various mathematical methods have been developed, such as the traditional approach which was proposed by Paulay in 1978 and calculates the ratio of the deflection at the ultimate limit state to the deflection at the elastic limit state of the tensile steel [18].

$$\mu = \frac{\Delta u}{\Delta y} \tag{4}$$

where μ , Δu , Δy refer to the ductility index, ultimate deflection, and yielding deflection, respectively.

The stiffness of a structural member is recognized as one of its fundamental properties. The resistance of a material to deformation under an applied force can be quantified using an index that represents its degree of deformation resistance. As shown in Figure 5, the initial and service stiffness of the tested concrete beams were evaluated. The findings indicate that increasing the shear reinforcement ratio enhances the stiffness of the concrete beams. Specifically, the control beam made of regular concrete had an initial stiffness of 58.59 kN/mm, which increased further after the inclusion of longer shear connectors.

The RC members possess inherent ductility and energy absorption capabilities, which enable the conversion of the mechanical energy into an internal potential energy. Additionally, these concrete members must contend with numerous complex processes, including the fracture mechanics governing concrete cracking and the deformations resulting from the elastic and plastic forces [19].

The findings on the energy absorption capacity are illustrated in Figure 5. The reference beam B2 was compared to the B1 beam, which was generated using U-shaped stirrups, and it was discovered that the energy absorption decreased to 1661 kN.mm, which is equivalent to 71% of B1. When the control beam B2 was compared to the other beams created with Z-shaped stirrups, the increase in energy absorption was found to be 6% for beam B6, which had a flange length of the stirrups equal to 50 mm.

VII. CRACK PATTERN AND FAILURE MODE

Table V shows the load that causes the first crack to appear in the beams. Compared to beam B1, the load was increased across the range, except for beams B4 and B6, where it was decreased by 10% and 7%, respectively. It was observed that the cracks initially emerged in the central region, with the load and onset of the cracking in the middle averaging 20% for all samples. This is attributed to the increased stresses in the middle due to the applied load, leading to the development and spread of the cracks upwards and sideways.

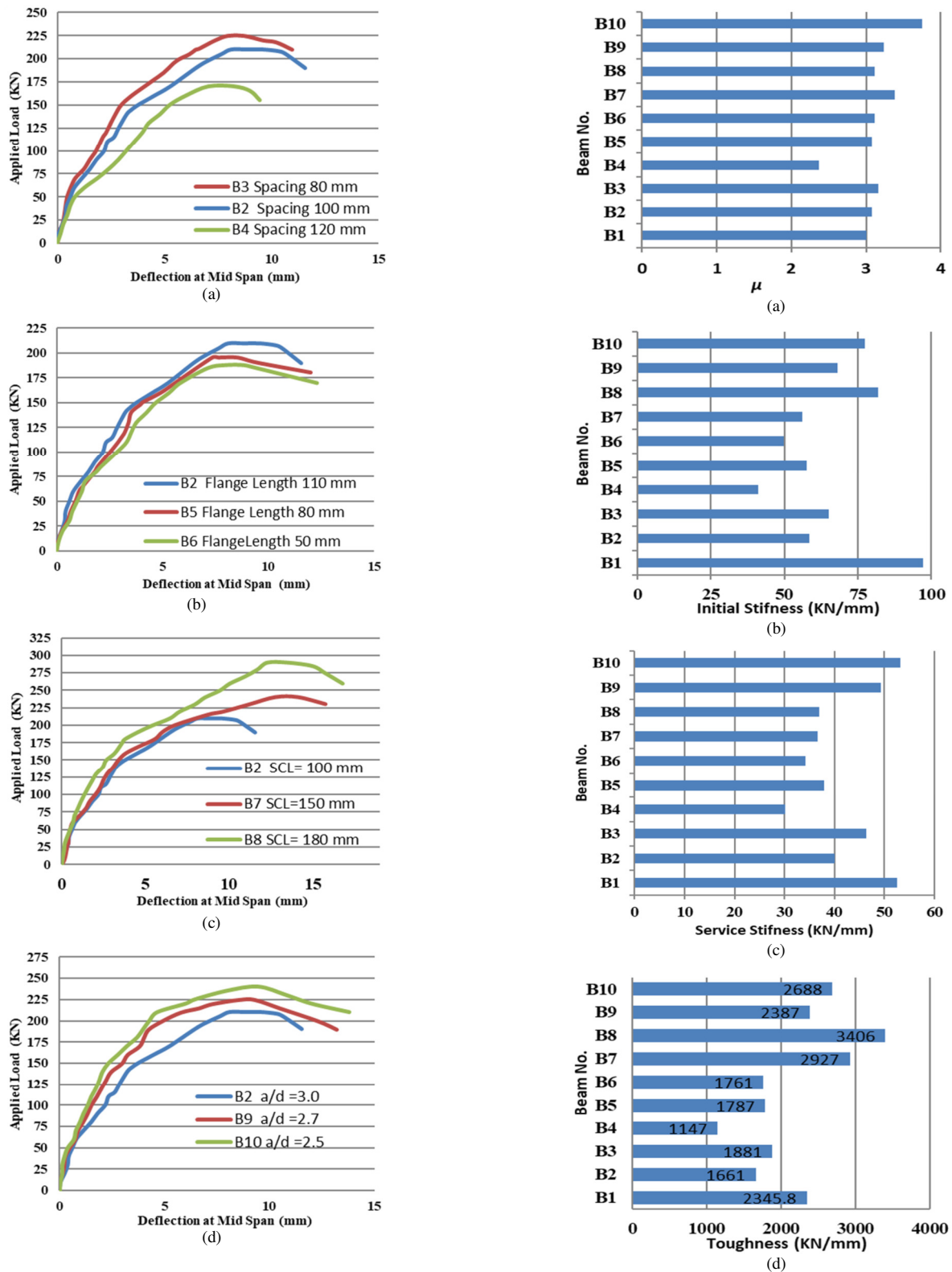


Fig. 4. Relation between the applied load and central deflection for (a) group A, (b) group B, (c) group C, and (d) group D. (a) Ductility ratio, (b) initial stiffness, (c) service stiffness, and (d) toughness.

A single failure pattern, namely shear failure, was observed in all the examined beams. The beams were initially designed to withstand greater bending than shear forces, and the addition

of an external steel plate was intended to enhance the bending capacity, but it resulted in a greater emphasis on studying the shear behavior of the beams, as depicted in Figure 6.

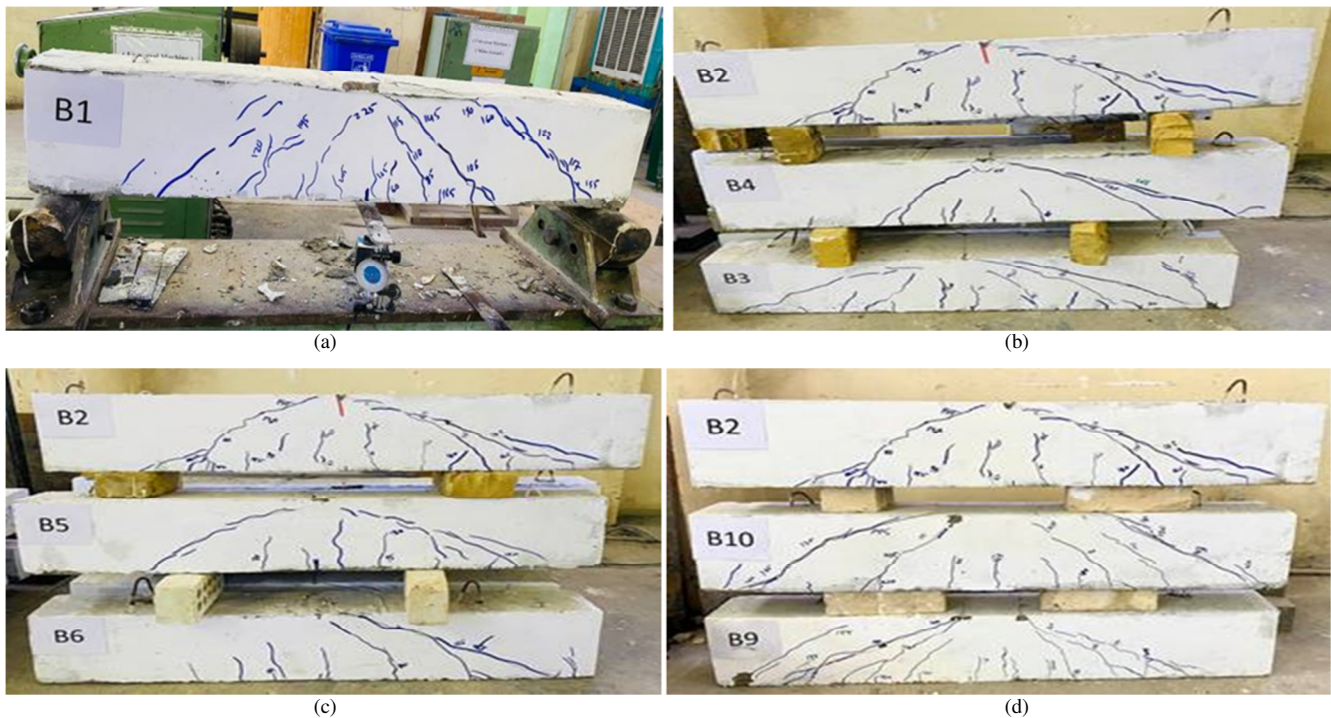


Fig. 5. Crack pattern and failure mode of the beams. (a) B1, (b) B2, B3, and B4, (c) B2, B5, and B6, and (d) B2, B9, and B10.

VIII. CONCLUSIONS

This study aims to examine the behavior of composite Self-Compacting Concrete (SCC) reinforced with an external steel plate and using Z-shaped stirrups instead of traditional stirrups. For this purpose, ten Reinforced Concrete (RC) beams were fabricated and subjected to monotonic tests under single and two-point loads. Additionally, two RC beams were produced for comparison purposes.

The Z-stirrup technique, with a spacing equal to 80% of the U-shaped stirrup spacing, exhibited approximately 90% of the shear capacity, aligning with the findings of [9]. The slight reduction in the ultimate load of the SCC beams was attributed to the decreased stiffness due to the shorter flange length of the Z-stirrups, while the transverse reinforcement strength contribution remained constant due to the consistent spacing between the Z-stirrups. Notably, the cracks first appeared in the central region, with the load and the onset of the crack in the middle averaging 20% for all samples, aligning with the observations of [7].

ACKNOWLEDGMENT

Great sincere appreciation to the College of Engineering, Mustansiriya University, for the facilitation of this research that its staff has shown.

REFERENCES

- [1] N. Mossahebi, A. Yakel, and A. Azizinamini, "Experimental investigation of a bridge girder made of steel tube filled with concrete," *Journal of Constructional Steel Research*, vol. 61, no. 3, pp. 371–386, Oct. 2004, <https://doi.org/10.1016/j.jcsr.2004.07.004>.
- [2] M. A. Shallal and A. M. K. A. Musawi, "Non-linear analysis of composite beam subjected to fire," *Journal of Engineering and Applied Science*, vol. 13, no. 22, pp. 9643–9650, 2018.
- [3] M. A. Shallal, A. M. Almusawi, K. A. Musawi, and F. Mussa, "Non-linear analysis of continuous composite beam subjected to fire," *International Journal of Civil Engineering and Technology*, vol. 9, no. 9, pp. 521–532, Sep. 2018.
- [4] N. A. Memon, M. A. Memon, N. A. Lakho, F. A. Memon, M. A. Keerio, and A. N. Memon, "A Review on Self Compacting Concrete with Cementitious Materials and Fibers," *Engineering, Technology & Applied Science Research*, vol. 8, no. 3, pp. 2969–2974, Jun. 2018, <https://doi.org/10.48084/etasr.2006>.
- [5] A. Shariati, "Various types of shear connectors in composite structures: A review," *International Journal of the Physical Sciences*, vol. 7, no. 22, pp. 2876–2890, Jun. 2012, <https://doi.org/10.5897/ijpsx11.004>.
- [6] T. A. Nguyen, N. M. Pham, T. C. Vo, and D. D. Nguyen, "Assessment of Shear Strength Models of Reinforced Concrete Columns," *Engineering, Technology & Applied Science Research*, vol. 12, no. 6, pp. 9440–9444, Dec. 2022, <https://doi.org/10.48084/etasr.5248>.
- [7] W. De Corte and V. Boel, "Effectiveness of spirally shaped stirrups in reinforced concrete beams," *Engineering Structures*, vol. 52, pp. 667–675, Apr. 2013, <https://doi.org/10.1016/j.engstruct.2013.03.032>.
- [8] K. A.-M. Mosheer and A. H. H. Hassoon, "Strengthening of Reinforced Concrete Beam in Shear Zone by Compensation the Stirrups with Equivalent External Steel Plates," *Journal of Babylon University*, vol. 24, no. 3, pp. 604–617, 2016.

- [9] A. S. Mahmood and S. M. Abd, "Effect of Bar Diameter on Shear Capacity of Reinforced Concrete Beams with Flamingo Shear Reinforcing technique," *Mathematical Statistician and Engineering Applications*, vol. 72, no. 1, pp. 719–729, Feb. 2023.
- [10] *IOS No.5: Portland Cement*, Central Agency for Standardization and Quality Control, Baghdad, Iraq, 2019.
- [11] *IOS No.45: Aggregate from Natural Sources for Concrete and Construction*, Central Agency for Standardization and Quality Control, Baghdad, Iraq, 1984.
- [12] *ACI 318-19: Building Code Requirements for Structural Concrete and Commentary*, American Concrete Institute, MI, USA, 2019.
- [13] Y. N. Ziraba, M. H. Baluch, I. A. Basunbul, A. M. Sharif, A. K. Azad, and G. J. Al-Sulaimani, "Guidelines Toward the Design of Reinforced Concrete (RC) Beams with External Plates," *American Concrete Institute*, vol. 91, no. 6, pp. 639–646, Jan. 1994, <https://doi.org/10.14359/1538>.
- [14] S. D. Jaafer, "Experimental Study to Investigate the Behavior of Self Compacting Axially Constrained Reinforced Concrete Deep Beams," MSc Thesis, Mustansiriyah University, Baghdad, Iraq, 2017.
- [15] *Specification and Guidelines for Self-Compacting Concrete*, European Federation Dedicated to Specialist Construction Chemicals and Concrete System, Brussels, Belgium, 2002.
- [16] *ACI237R-07: Self Consolidating Concrete*, American Concrete Institute, MI, USA, Apr. 2017.
- [17] F. E. Ame, J. N. Mwero, and C. K. Kabubo, "Openings Effect on the Performance of Reinforced Concrete Beams Loaded in Bending and Shear," *Engineering, Technology & Applied Science Research*, vol. 10, no. 2, pp. 5352–5360, Apr. 2020, <https://doi.org/10.48084/etasr.3317>.
- [18] T. Paulay, "A consideration of P-delta effects in ductile reinforced concrete frames," *Bulletin of the New Zealand Society for Earthquake Engineering*, vol. 11, no. 3, pp. 151–160, Sep. 1978, <https://doi.org/10.5459/bnzsee.11.3.151-160>.
- [19] A. N. Hanoon, A. A. Abdulhameed, H. A. Abdulhameed, and S. K. Mohaisen, "Energy Absorption Evaluation of CFRP-Strengthened Two-Spans Reinforced Concrete Beams under Pure Torsion," *Civil Engineering Journal*, vol. 5, no. 9, pp. 2007–2018, Sep. 2019, <https://doi.org/10.28991/cej-2019-03091389>.